THE JOURNAL OF BIOLOGICAL CHEMISTRY VOL. 285, NO. 20, pp. 15256–15267, May 14, 2010

Hormone Binding and Co-regulator Binding to the Glucocorticoid Receptor are Allosterically Coupled[S]

Received for publication, January 26, 2010, and in revised form, March 9, 2010 Published, JBC Papers in Press, March 24, 2010, DOI 10.1074/jbc.M110.108118

Samuel J. Pfaff[‡] **and Robert J. Fletterick**[§1]

From the [‡]*Graduate Group in Biophysics and the* [§]*Department of Biochemistry and Biophysics, University of California, San Francisco, California 94143*

The glucocorticoid receptor initiates the cellular response to glucocorticoid steroid hormones in vertebrates. Co-regulator proteins dock to the receptor in response to hormone binding and potentiate the transcriptional activity of the receptor by modifying DNA and recruiting essential transcription factors like RNA polymerase II. Hormones and co-regulators bind at distinct sites in the ligand binding domain yet function cooperatively to mediate transcriptional control. This study reveals and quantifies energetic coupling between two binding sites using purified components. Using a library of peptides taken from co-regulator proteins, we determine the pattern of co-regulator binding to the glucocorticoid receptor ligand binding domain. We show that peptides from co-regulators differ in their effects on hormone binding and kinetics. Peptides from DAX1 and SRC1 bind with similar affinity, but DAX1 binding is coupled to hormone binding, and SRC1 is not. Mechanistic details of co-regulator binding and coupling to the hormone binding pocket are uncovered by analysis of properties endowed by mutation of a key residue in the allosteric network connecting the sites.

Vertebrate endocrine signaling by steroids is primarily mediated by the steroid receptor (SR)[2] class of nuclear receptors (1). SRs affect biological outcomes by regulating target gene mRNA levels through transcriptional activation and active repression. The glucocorticoid (GC) steroids are the primary stress hormones released by hypothalamic-pituitary-adrenal axis in humans and regulate numerous physiological processes, including homeostasis, cell differentiation, apoptosis, and metabolism (2, 3). Disruption of GC signaling is a component of many diverse disease states, including depression, leukemia, and asthma. Natural and synthetic GCs are among the most prescribed drugs for their anti-inflammatory and immune-suppressive profiles. However, long term GC treatment may result in severe side effects including diabetes, glaucoma, and osteoporosis (2–4).

The first localized step in translating a glucocorticoid signal toward a genomic outcome is the binding of GC to the glucocorticoid receptor (GR) in the cytosol. In the absence of hormone, GR is sequestered outside the nucleus where it is stabilized by regulatory complexes of chaperone proteins, which include Hsp90, Hsp70, Hsp40, HOP, and p23 (5–7). Interaction with this complex is required for high affinity ligand binding to GR and all other SRs (8, 9). After ligand binding, GR is transported to the nucleus (9–13), where it initiates a multistep series of events that are cell- and tissue-specific programs of gene activation and repression (14–19).

GR is a modular scaffolding protein, consisting of three major functional domains. The N-terminal 400 residues comprise a mostly unstructured region that harbors a transcriptional activation region dubbed activation function 1 (AF-1). AF-1 can bind co-regulator proteins, and its transcriptional activity is not ligand-dependent (20, 21). Residues 430–500 compose a direct DNA binding domain that is the most well conserved domain across all nuclear receptors (NRs) (22–24). GR forms homodimers through this domain and uses zinc finger motifs coded in this region to recognize and bind specific glucocorticoid binding sequences associated with target genes on DNA (25). Interestingly, a recent study elucidated a role for the DNA binding domain and the specific glucocorticoid binding sequence to which it is bound in allosteric, interdomain communication through the receptor (26).

The C-terminal 250 residues of GR encompass the ligand binding domain (LBD), which initiates the cell response to GCs. GR preference for its natural hormone cortisol evolved through mutations in the LBD ~400 million years ago when it diverged from the mineralocorticoid receptor (27). Interestingly, the molecular basis of its evolved specificity involves mutations at the receptor-hormone interface as well as sets of permissive mutations to other regions of the LBD shown to be critical in stabilizing a functional receptor conformation (27–29). Well conserved through the nuclear receptor superfamily, the LBD is a three-layered α-helical sandwich structure whose hydrophobic core is completed by lipophilic hormone binding to the protein interior (30–32). The surface of the nuclear receptor LBD typically contains at least two protein-protein interaction sites; they are a dimerization surface, more prevalent in the class II receptors (thyroid hormone receptor, vitamin D receptor, retinoic acid receptor) that are regulated by forming heterodimers with retinoid X receptor (33), and a co-regulator protein docking site, termed activation function-2 (AF-2). Composed of residues from helices 3, 4, 5, and 12, AF-2 is a shallow, mainly hydrophobic groove surrounded by polar residues that allows for specific docking of co-regulators to the LBD surface (34–36).

[S] The on-line version of this article (available at http://www.jbc.org) contains supplemental Figs. S1 and S2.

[1] To whom correspondence should be addressed. Tel.: 415-476-5080; Fax: 415-476-1902; E-mail: robert.fletterick@ucsf.edu.

[2] The abbreviations used are: SR, steroid receptor; GC, glucocorticoid; GR, glucocorticoid receptor; AF, activation function 1; NR, nuclear receptors; LBD, ligand binding domain; TCEP, Tris(2-carboxyethyl)phosphine; dex, dexamethasone; dex-fl, fluorescein-labeled dex; FP, fluorescence polarization; CHAPS, 3-[(3-cholamidopropyl)dimethylammonio]-1-propanesulfonic acid; ER, estrogen receptor; mP, millipolarization units; SMRT, silencing mediator of retinoic acid and thyroid hormone receptor.

Co-regulators are essential players in the transduction of hormone signals through nuclear receptors (37–39). Canonically, ectopic expression of co-activators, including the p160 family (40–42), leads to an enhancement of target gene expression upon hormone treatment, whereas co-repressors such as NCoR and SMRT silence hormone-induced gene expression (43). The intrinsic functionality of co-regulators is varied, with many implicated in chromatin remodeling and recruitment of the basal transcription machinery (44, 45). As their docking to nuclear receptors typically follows ligand binding and subsequent localization to the nucleus, co-regulators represent a vital, cell-specific layer of control that can be employed to modify the cellular response to hormone.

Both co-activators and co-repressors interact with NR LBDs by docking short, amphipathic, helical segments at the AF-2 surface (34, 46). Many co-regulators contain several of these NR interaction sites, referred to henceforth as NR boxes. The canonical co-activator NR box is composed of the sequence L*XX*LL, where L is leucine, and *X* is any amino acid. The most well characterized co-activators, the p160 family (40–42, 47–49), each contain at least three NR boxes that share the L*XX*LL core but differ in the residues at the +2 and +3 positions in addition to the flanking sequence. These residues have been shown to be key determinants of selectivity between co-regulators and the wide array of NRs with which they interact (50). Several studies have determined patterns of co-regulator binding to NR LBDs by structural, biochemical, or cell-based methods (51–56). Interestingly, many NRs assayed show different patterns of co-regulator binding based on the identity of the ligand in the binding pocket, implying allosteric coupling between the two sites.

This report presents the first quantitative assessment of coupling between GR LBD key functional sites. Allosteric modulation of ligand binding kinetics by co-regulators at the AF-2 surface is revealed and characterized using fluorescence polarization (FP). A similar technique is applied to determine and quantify the pattern of co-regulator binding to agonist-bound GR LBD using a library of 18 NR box peptides from physiologically important co-regulators. Additionally, the mechanism of action of a recently discovered mutation with profound functional consequences in the cell is elucidated (57). Together these results represent a first step in the development of a quantitative framework for the description of coupling between the co-regulator docking site and the ligand binding site.

MATERIALS AND METHODS

Protein Expression and Purification—Human GR LBD (520–777, F602S, C638D with/without M752I) was expressed as a His_6 fusion protein from a modified pACYCDuet vector in *Escherichia coli* strain BL21Star. The encoded GR sequence was optimized for expression in *E. coli* (GeneArt, Burlingame, CA). Expression and purification were carried out as described (58). Thrombin cleavage of the His_6 tag was carried out during dialysis into storage buffer containing 20 mM HEPES, pH 7.4, 150 mM NaCl, 10% glycerol, 0.2 mM TCEP, 0.04% CHAPS, 10 μM dexamethasone.

Ligand Removal—Ligand-free GR for fluorescence studies was prepared in two manners. For GR_{SD} (F602S, C638D), ligand removal was accomplished by passage over a NAP-25 desalting column (GE Healthcare). For GR_{M752I} (F602S, C638D, M752I), dialysis into storage buffer without dexamethasone followed by passage over a NAP-25 column was necessary.

NR Box Peptide Library—NR box peptides were obtained from Elim Biopharmaceuticals (Hayward, CA) with the exception of SRC1-3 and SRC3-3, which were generous gifts of Dr. R. K. Guy. SRC1-3 and SRC3-3 each contain a non-native N-terminal cysteine residue to allow for easy coupling of fluorescent probes. All other NR box sequences are wild type. Peptide sequences are as follows: SRC1-2, CPSSHSSLTERHKILHRLLQEGSPS; SRC1-3, CESKDHQLLRYLLDKDEKDL; SRC1-4, AQQKSLLQQLLTE; SRC2-1, SKGQTKLLQLLTCSS; SRC2-2, KHKILHRLLQDSS; SRC2-3, KENALLRYLLDKDD; SRC3-3, CKKENNALLRYLLDRDDPSD; PGC1α-1, EPSLLKKLLLAPAN; ARA70-2, TSEKFKLLFQ; Hsp90-1, NLCKIMKDILEK; Hsp90-2, GWTANMERIMKAQ; DAX1-1, QWQGSILYNMLMSAK; DAX1-2, PRQGSILYSMLTSAK; DAX1-3, PRQGSILYSLLTSSK; SHP-1, ASHPTILYTLLSPGP; SHP-2, APVPSILKKILLEEPNS; SMRT-1, RVVTLAQHISEVITQDYTR; SMRT-2, TNMGLEAIIRKALMGKYD.

Fluorescence Polarization Kinetics—All fluorescence polarization experiments were carried out in black, non-binding surface, 384-well plates (Corning) in a buffer containing 20 mM HEPES, pH 7.4, 150 mM NaCl, 0.2 mM TCEP, 0.04% CHAPS at room temperature. Kinetic measurements were performed on a SpectraMax M5 plate reader (Molecular Devices). For association measurements, GR was incubated with the specified peptide for 15 min at room temperature followed by the addition of dexamethasone-fluorescein (Invitrogen) at $t = 0$. Final concentrations of components were 1 μM GR, 10 μM peptide, and 20 nM dexamethasone-fluorescein. Timed measurements were taken typically every 30 s or 1 min until after the reaction had reached equilibrium. Dissociation was initiated by the addition of 50 μM unlabeled dexamethasone, and measurements were taken until equilibrium was reached. Data were fit using nonlinear regression to one-phase association or one-phase decay models in Prism 5 (GraphPad Software). All values reported represent the mean ± S.E. of at least three independent experiments.

Fluorescence Polarization Affinity—All fluorescence polarization experiments were carried out in black, non-binding surface, 384-well plates (Corning), in a buffer containing 20 mM HEPES, pH 7.4, 150 mM NaCl, 0.2 mM TCEP, 0.04% CHAPS at room temperature. 1 μM GR_{SD} or 500 nM GR_{M752I} was incubated with 40 nM fluorescein-labeled dexamethasone (dex-fl) until equilibrium was reached. GR·dex-fl was diluted 1:1 into samples of peptide from 200 μM to 30 nM prepared by serial dilution. Final concentrations of components were 500 nM GR_{SD}, 20 nM dex-fl, 100 μM–15 nM peptide or 250 nM GR_{M752I}, 20 nM dex-fl, 50 μM–7.5 nM peptide. Steady-state affinity measurements were performed on an Analyst AD, Analyst HT, or SpectraMax M5 plate reader (Molecular Devices). Data were fit by nonlinear regression to a one-site saturation binding model in Prism 5 (GraphPad Software). All values reported represent the mean of at least three independent experiments.

Fluorescent NR Box Probes—SRC1-3 and SRC3-3 peptides were synthesized with a non-native cysteine at the N terminus to allow easy coupling to fluorescent probes (51). Maleimide-Alexa Fluor 555 (Invitrogen) was coupled to each peptide in 20

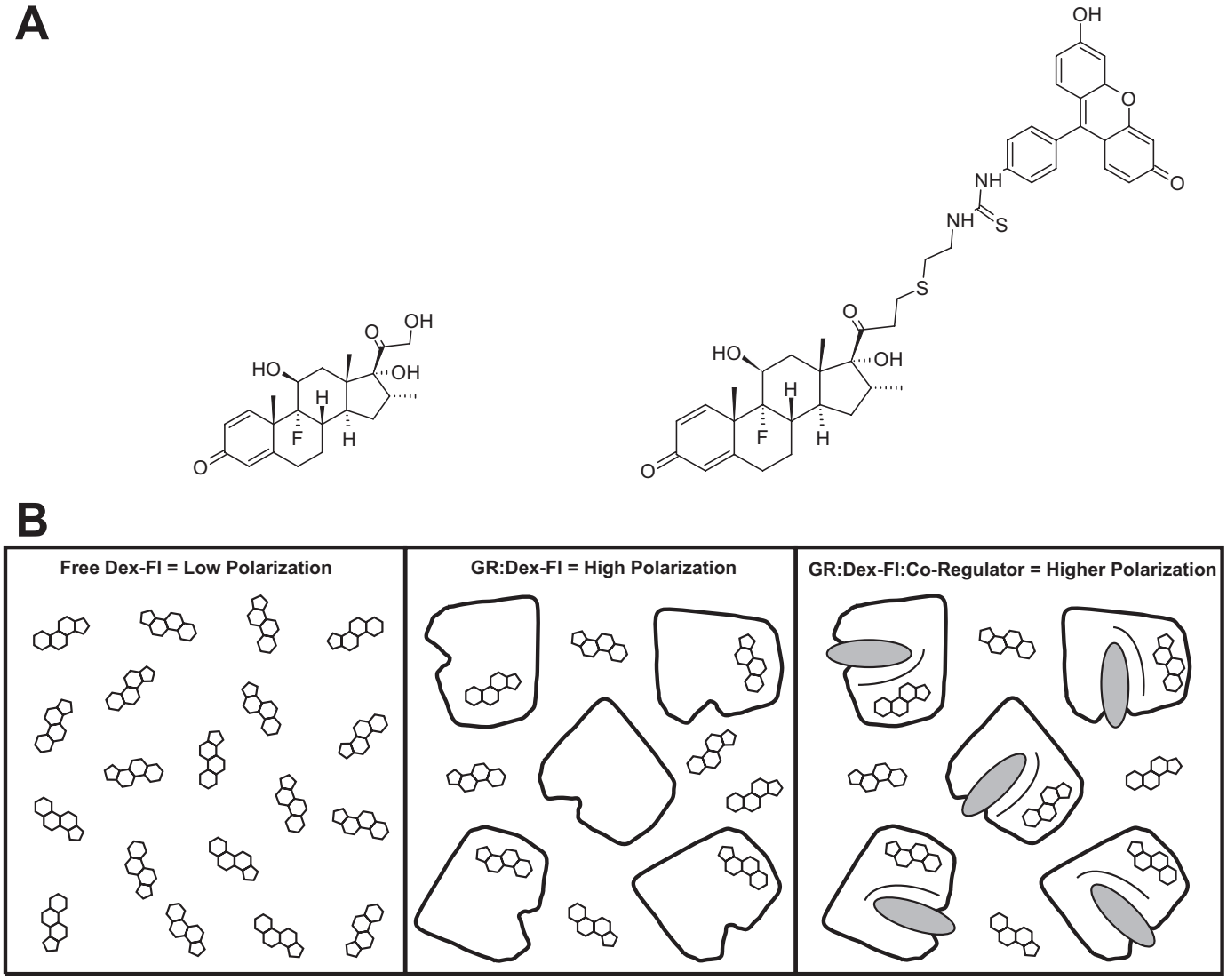

FIGURE 1. *A*, dexamethasone (*left*) and dexamethasone-fluorescein (*right*) are shown. *B*, schematics depicting the interactions observable by fluorescence polarization with dex-fl are shown. dex-fl (*ring structure*) binds GR (*large shape*) yielding high polarization. Co-regulator peptide (*gray oval*) binds GR·dex-fl, and binding is affected through allostery, further increasing dex-fl polarization.

mM HEPES, pH 7.1, 0.4 mM TCEP at room temperature for 3 h. The reaction was quenched with β-mercaptoethanol, and the peptides were separated from free probe using a Superdex Peptide column on an Akta Explorer FPLC (GE Healthcare). Peptide concentration was determined using $\lambda = 280$ nM absorbance, with the appropriate correction factor applied to account for the Alexa Fluor 555 contribution to the signal. Binding measurements were made in either FP buffer (20 mM HEPES, pH 7.4, 150 mM NaCl, 0.04% CHAPS, 0.2 mM TCEP) or FP plus 10 μM dex at room temperature on a SpectraMax M5 plate reader (Molecular Devices). NR box-fluor, present at 20 nM in all wells, was titrated with GR from 10 μM to 4.5 nM. Isotherms were analyzed and fit by nonlinear regression to a single-site saturation binding model in Prism 5 (GraphPad Software). All values reported represent the mean ± S.E. of at least three independent experiments.

RESULTS

GR Ligand Binding Kinetics—Crystal structures show a spectrum of physical interactions of GR LBD with peptides, drugs, and self (59–63). However, quantitative evaluation of these interactions and their relationships is scant. Biochemical interrogation of GR LBD and its various interaction partners has long been hindered by difficulty in obtaining stable, functional receptors for *in vitro* studies. The majority of published work using recombinantly expressed GR LBD, including this study, has been aided by incorporation of solubility-enhancing mutations discovered by yeast screens of GR activity (58, 59, 64),[3] and GR containing the mutations F602S and C638D will be referred to henceforth as GR_{SD}.

To assess the functionality of purified GR LBD, binding kinetics of dex-fl (Fig. 1*A*) were measured using fluorescence polarization (Fig. 2). dex-fl is a fluorescent analogue of the potent, synthetic GC dexamethasone that has been shown to bind GR with a similar affinity (65). To facilitate this ligand binding study, unlabeled dex remaining from the protein preparation was removed from solution through dialysis or desalt-

[3] B. Darimont, unpublished results.

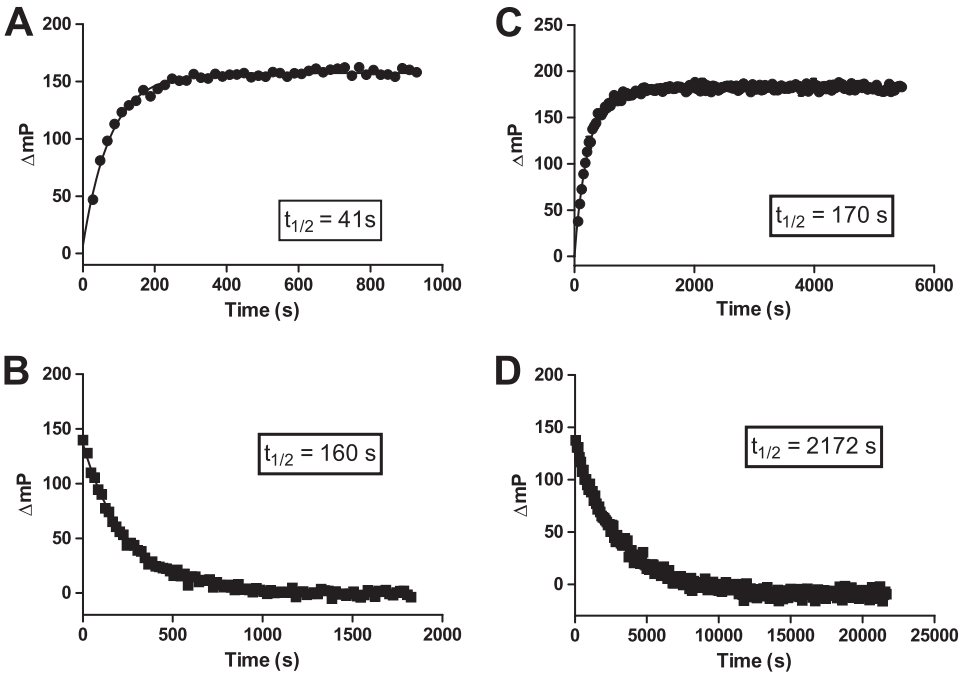

FIGURE 2. **GR·dex-fl binding kinetics.** *A*, 1 μM GR_{SD} (F602S, C638D), 20 nM dex-fl association is monitored by fluorescence polarization. *B*, 1 μM GR_{SD}, 20 nM dex-fl dissociation induced by the addition of 50 μM unlabeled dex is shown. *C*, 1 μM GR_{M752I}, 20 nM dex-fl association is shown. *D*, 1 μM GR_{M752I}, 20 nM dex-fl dissociation. All data fit to one-phase exponential models to yield half-times.

ing. Previous studies (58, 60, 64) have shown that recombinantly expressed GR LBD can readily exchange ligand under non-denaturing conditions, in sharp contrast with the androgen receptor,[4] suggesting ligand binding pocket accessibility may be a feature of GR. Fig. 2, *A* and *B*, shows association and dissociation of the GR_{SD}·dex-fl complex monitored to equilibrium. Both processes were fit to a single exponential model that yielded half-times of 41 and 160 s at 25 °C for association and dissociation, respectively.

NR Box Peptides Slow Ligand Binding—Previous studies have shown NR box peptides have a stabilizing effect on the AF-2 regions of NRs (66–69). Reflecting this, several NRs, including GR and mineralocorticoid receptor, require addition of NR box peptides to obtain complexes stable enough for crystallographic study (61, 70). Helix 12 and other structural elements that form the AF-2 binding site have been postulated to form a lid on the ligand binding pocket (71). This encouraged us to evaluate the functional interplay between NR box binding to GRs AF-2 and dex-fl binding to the ligand binding pocket using FP kinetics.

GR was incubated with a 10× molar excess of each of 18 physiological NR box peptides and was then assayed for binding to dex-fl (Fig. 3, Table 1). Association of the GR_{SD}·dex-fl complex in the presence of peptides from the DAX1 co-repressor and SRC2 co-activator are shown in Fig. 3*A*. Both peptides alter two components of the exponential association process; the binding plateau is heightened, and time to equilibrium is extended, 5-fold for SRC2-3 and 6-fold for DAX1-3. Fig. 3*C* shows $t_{½}$ values for GR_{SD}·dex-fl complex formation in the presence of peptides from our NR box library. Many NR box peptides showed little influence on the on-rates of the hormone analog, but large changes in rates were found for SRC1-4, SRC2-3, SRC3-3, PGC1α-1, DAX1-2, DAX1-3, and SHP-2, indicating that peptide residence at AF-2 affects the ligand binding pocket. To confirm the binding through a direct measure, isothermal titration calorimetry experiments were carried out with interacting peptide SRC1-4 and GR showing a strong interaction (data not shown). A more dramatic effect was observed during dissociation of the GR·dex-fl complex (Fig. 3, *B* and *D*), initiated by the addition of 50 μM unlabeled dex. In this library SRC2-3 and DAX1-3 slowed ligand dissociation by 10- and 27-fold, respectively (Fig. 3*B*). This biased modulation of dissociation kinetics was apparent for all NR box peptides that affected ligand binding (Fig. 3, *C* and *D*, Table 1).

M752I Throttles GR Ligand Binding—In a recent study Ricketson *et al.* (57) identified several mutations of the GR LBD that increase responsiveness to dex while also reducing the receptor dependence on ubiquitous molecular chaperone Hsp90. One of the mutations identified was M752I, which in addition to the aforementioned effects was shown to increase GR affinity for co-regulator SRC2. Structurally, Met-752 is positioned at a key location for inter- and intraprotein interactions (59). At the N terminus of helix 12, it directly contacts bound NR box peptides at its −1 position, a conserved hydrophobic residue, and packs against hydrophobic side chains from residues in neighboring helices of the receptor. Methionine side chains are both hydrophobic and flexible. Receptors naturally possessing a more constrained Leu at this position, including those for thyroid hormone, retinoic acid, and vitamin D, typically do not depend on Hsp90 in the unliganded state. These receptors are localized to the nucleus in the absence of ligand and are regulated by the nuclear receptor RXR through heterodimerization (33, 72–74). Fig. 2, *C* and *D*, shows association and dissociation of dex-fl from GR_{M752I}. Both processes were fit to a single exponential model that yielded half-times of 170 and 2172 s, respectively, for association and dissociation. Thus, mutation of a flexible, hydrophobic surface residue 10 Å from the dex-fl molecule slowed both processes, with a greater impact being observed on dissociation, suggesting the amino acid residue at position 752 affects ligand binding pocket stability through a mechanism likely similar to that shown by NR box binding.

M752I AF-2 Binding Preferentially Slows Hormone Association—NR box modulation of dex-fl binding kinetics was also explored with GR_{M752I}. Interacting NR box peptides produced highly stable complexes, with $t_{½}$ association as high as 9,400 s (*DAX1-3*; Fig. 4, *A* and *C*) and $t_{½}$ dissociation reaching 74,000 s

[4] S. J. Pfaff and R. J. Fletterick, unpublished results.

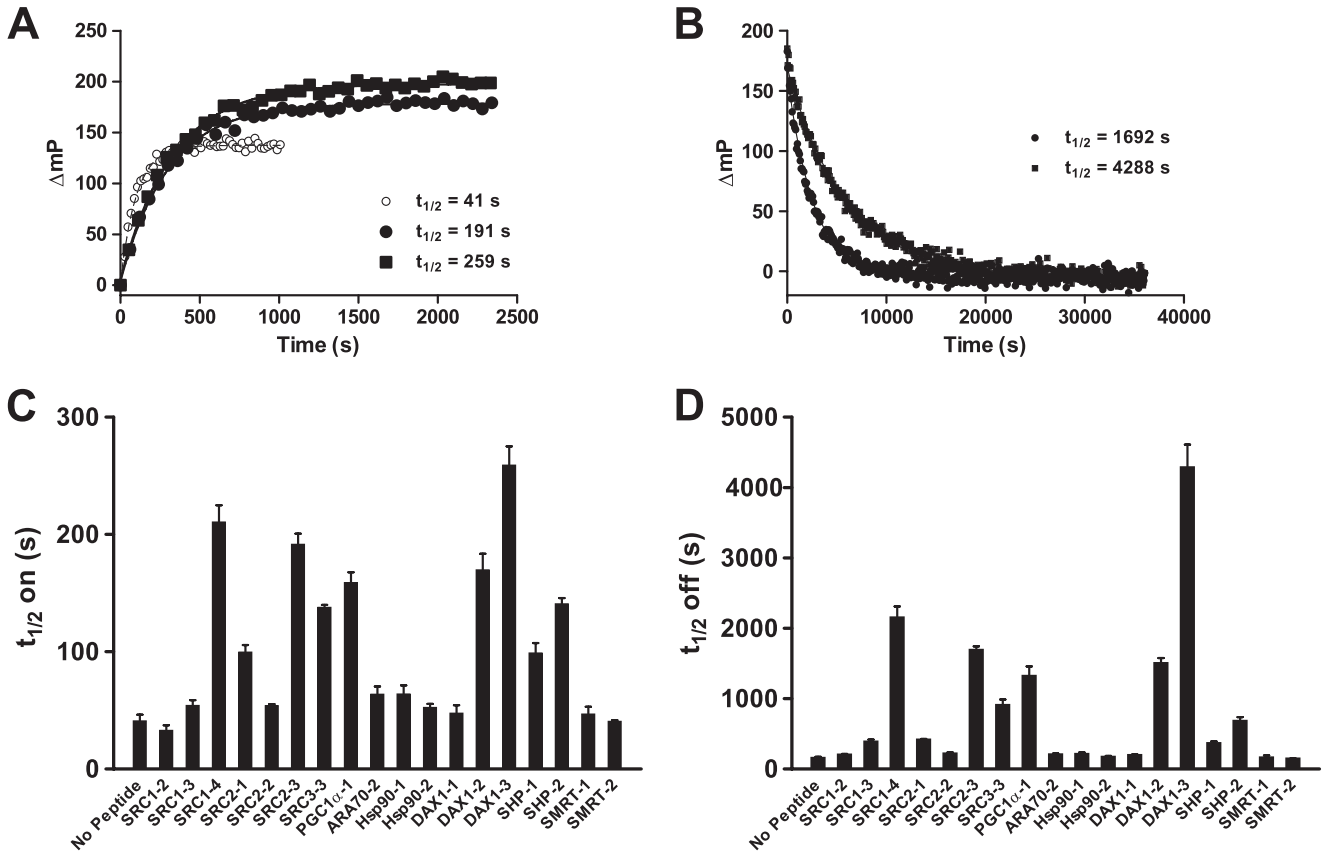

FIGURE 3. **NR box binding is coupled to ligand binding kinetics.** *A*, 1 μM GR_{SD}, 20 nM dex-fl association in the presence of 10 μM SRC2-3 (*circles*), DAX1-3 (*squares*), and no NR box (*gray circles*) is shown. Base-line-subtracted data fit to one-phase exponential model. *Error bars* are omitted for clarity. *B*, half-times of GR_{SD}·dex-fl association in the presence of 10 μM NR box are shown. *C*, 1 μM GR_{SD}, 20 nM dex-fl dissociation in the presence of 10 μM SRC2-3 (*circles*) and DAX1-3 (*squares*) is shown. *D*, half times of GR_{SD}·dex-fl dissociation in the presence of 10 μM NR box are shown.

TABLE 1

Half-times of association and dissociation of the GR·dex-fl complex

Bold numbers represent -fold half-time increase over no peptide condition.

NR box peptide	GR_{SD}				GR_{M752I}			
	$t_{½}$ on	-Fold increase	$t_{½}$ off	-Fold increase	$t_{½}$ on	-Fold increase	$t_{½}$ off	-Fold increase
	s		*s*		*s*		*s*	
No peptide	41	**1**	160	**1**	170	**1**	2172	**1**
SRC1-2	33	**1**	206	**1**	301	**2**	3931	**2**
SRC1-3	54	**1**	392	**2**	668	**4**	6326	**3**
SRC1-4	211	**5**	2152	**13**	3078	**18**	41069	**19**
SRC2-1	100	**2**	418	**3**	471	**3**	4887	**2**
SRC2-2	54	**1**	222	**1**	312	**2**	3455	**2**
SRC2-3	192	**5**	1692	**11**	3143	**18**	29273	**13**
SRC3-3	138	**3**	910	**6**	2265	**13**	18907	**9**
PGC1α-1	159	**4**	1325	**8**	2341	**14**	31007	**14**
ARA70-2	64	**2**	207	**1**	281	**2**	2444	**1**
Hsp90-1	64	**2**	215	**1**	292	**2**	2613	**1**
Hsp90-2	53	**1**	175	**1**	188	**1**	1622	**1**
DAX1-1	48	**1**	198	**1**	264	**2**	2790	**1**
DAX1-2	170	**4**	1506	**9**	3193	**19**	28890	**13**
DAX1-3	259	**6**	4288	**27**	9452	**56**	73949	**34**
SHP-1	99	**2**	368	**2**	1432	**8**	10301	**5**
SHP-2	141	**3**	683	**4**	2295	**13**	17496	**8**
SMRT-1	47	**1**	165	**1**	244	**1**	2021	**1**
SMRT-2	41	**1**	150	**1**	225	**1**	1588	**1**

(*DAX1-3*; Fig. 4, *B* and *D*). Dex-fl dissociation was not monitored to equilibrium for reactions with strong interacting peptides, as the time required to reach a lower plateau was too long to ensure high protein quality for the duration of the assay. To acquire an estimate of the $t_{½}$ in this situation, we measured the reaction for typically at least 50,000 s and extrapolated the fit curve to a lower polarization plateau of 20 mP. Data sets for SRC1-4, SRC2-3, PGC1α-1, DAX1-2, and DAX1-3 were treated this way. Strikingly, the effect of NR box on ligand association and dissociation rates was reversed from GR_{SD} in the context of M752I, with the peptide having greater influence on dex-fl association (Table 1).

To test the hypothesis that NR box peptides have more affinity for unliganded GR_{M752I}, SRC3-3 was covalently labeled with

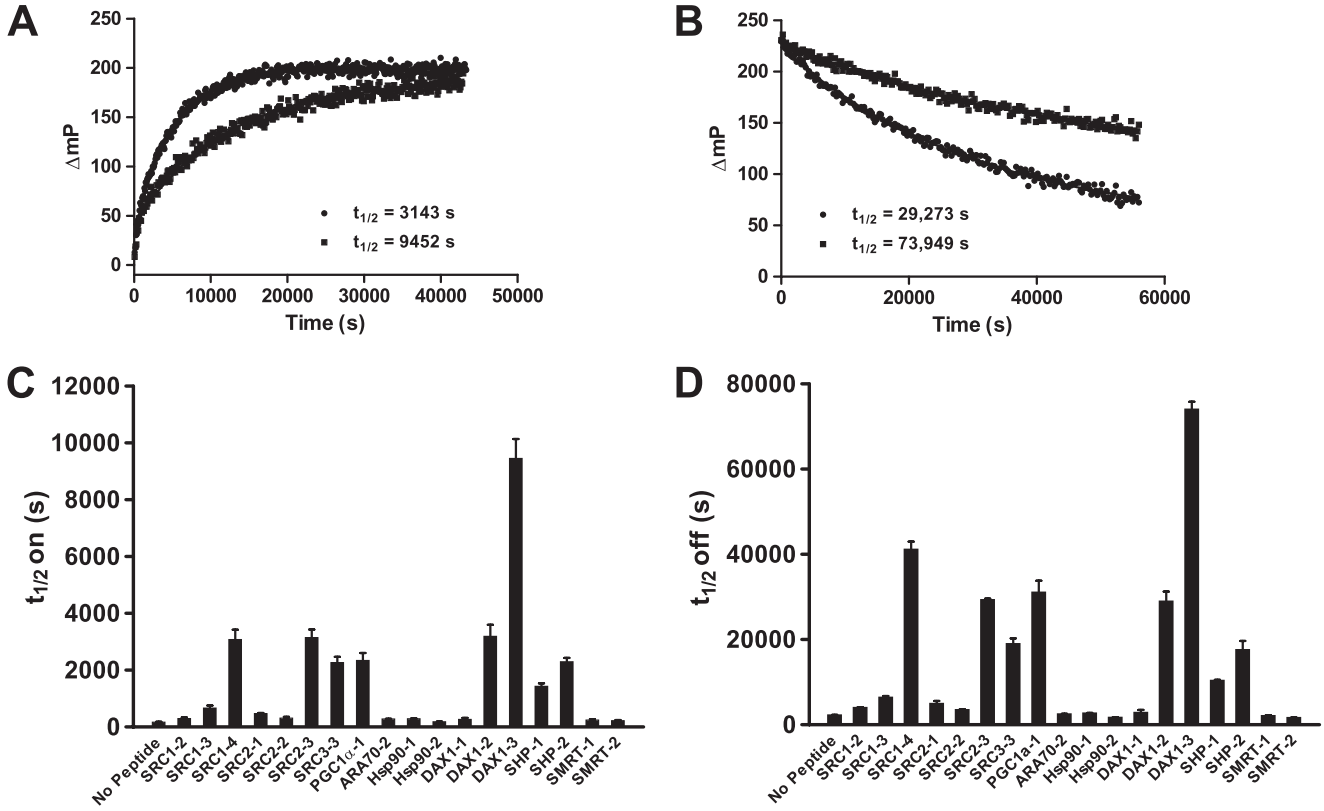

FIGURE 4. **GR_{M752I}·dex-fl binding kinetics in the presence of NR box peptides.** *A*, 1 μM GR_{M752I}, 20 nM dex-fl association in the presence of 10 μM SRC2-3 (*circles*) and DAX1-3 (*squares*) is shown. Base-line-subtracted data fit to a one-phase exponential model. *B*, half-times of GR_{M752I}·dex-fl association in the presence of 10 μM NR box are shown. *C*, 1 μM GR_{M752I}, 20 nM dex-fl dissociation in the presence of 10 μM SRC2-3 (*circles*) and DAX1-3 (*squares*) is shown. *D*, half-times of GR_{M752I}·dex-fl dissociation in the presence of 10 μM NR box are shown.

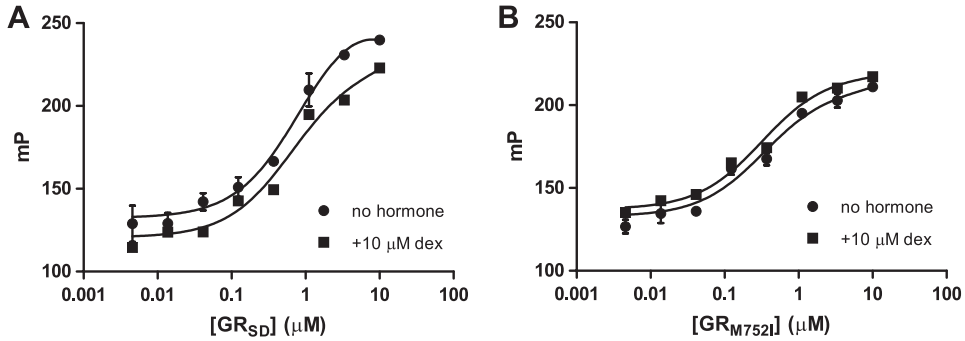

FIGURE 5. **GR binding to SRC3-3-fluor with and without dex.** *A*, GR_{SD} titrated against 20 nM SRC3-3 conjugated to Alexa-Fluor 555 in the presence (*circles*) or absence (*squares*) of 10 μM dex is shown. *B*, GR_{M752I} titrated against 20 nM SRC3-3 conjugated to Alexa-Fluor 555 in the presence (*circles*) or absence (*squares*) of 10 μM dex is shown.

Alexa Fluor 555 through its N-terminal cysteine for direct-binding fluorescence polarization measurements (Fig. 5) (51, 52). In the presence of 10 μM dex, GR_{M752I} bound SRC3-3-fluor with a K_D = 349 ± 22 nM (Fig. 5*B*). GR_{M752I} that had been stripped of ligand bound SRC3-3-fluor with a nearly identical K_D of 327 ± 33 nM, indicating that both holo- and apoGR_{M752I} present interaction-competent AF-2 surfaces. For comparison, the analogous experiments were carried out with GR_{SD} SRC3-3-fluor-bound apo- and holo-GR_{SD} similarly, with a K_D = 676 ± 61 nM for apo- and a K_D = 741 ± 61 nM for dex-bound GR_{SD} (Fig. 5*A*). Thus, each GR binds this peptide nearly as well with or without hormone but the stronger interaction is with GR_{M752I}.

Determination of NR Box Binding Affinities by FP—NR box binding to AF-2 alters the plateau in polarization in addition to the kinetics of GR·dex-fl complex formation (Fig. 3*A*). This finding allowed determination of NR box binding affinities using dex-fl polarization as a readout. A major source of this enhanced polarization signal is likely an increase in the affinity of dex-fl for GR as a function of co-regulator peptide bound at AF-2. As polarization is a composite signal influenced by physical and chemical factors affecting the fluorophore, the potential contributions of other sources to the enhanced polarization observed cannot be discounted. Titrations of NR box peptide were performed against constant concentrations of GR and dex-fl, yielding K_D values for 8 of 18 peptides tested (Table 2, supplemental Fig. S1). Example titration curves representing the various binding modes observed are shown in Fig. 6.

NR box binding to GR occurred in six distinct modes: high plateau saturable binding (*a*), low plateau saturable binding (*b*), non-saturable binding (*c*), weak binding (*d*), no binding (*e*), and co-repressor binding (*f*). As expected, NR box peptides identified as having the greatest effect on ligand binding kinetics were

primarily those that displayed saturable binding behavior. K_D values for these peptides are listed in Table 2. Of these NR box peptides, four belong to the p160 family of co-activators (SRC1-3, SRC1-4, SRC2-3, SRC3-3), whereas the others (PGC1α-1, DAX1-2, DAX1-3, and SHP-2) represent different families of co-regulators. PGC1α-1 is derived from a co-activator, whereas the remaining NR box peptides come from the unusual nuclear receptors/co-repressors DAX1 and SHP. SHP contains a putative LBD and has no identified ligand; the structure of DAX1 C-terminal 230 amino acids shows a nearly complete LBD with no hormone binding pocket (74). Both are implicated in GR signaling in an NR box-dependent manner (75, 76). DAX1 and SHP are thought to silence NR-mediated transcription by competing with co-activators for binding to AF-2, and each appears to contain multiple NR box peptides with affinity for GR. In the case of the nuclear receptor LRH-1, DAX1 NR boxes were not implicated in repression of transcription, and a different motif was identified (74). SHP-1 peptide showed non-saturable binding behavior (Fig. 6*C*) yet had a significant effect on ligand binding, suggesting moderate (>10 μM) affinity for GR (Table 1). DAX1-3 bound well to GR with K_D of 1–2 μM. However, its relative advantage in K_D does not appear great enough to explain its exaggerated effect on dex-fl binding kinetics (Figs. 3 and 4 and Table 1). Together these observations imply either a unique binding mode or multiple binding sites for this peptide.

TABLE 2

NR box peptide dissociation constants

Confidence interval (CI) values were determined by fitting to a one-site saturation binding model. Values reported are the averages of at least three independent experiments.

NR box	GR_{SD} K_D, 95% CI	GR_{M752I} K_D, 95% CI	-Fold decrease
	μM	μM	
SRC1-3	1–2	0.6–2.0	1
SRC1-4	1–3	0.2–0.7	5
SRC2-3	2–4	0.2–0.5	7
SRC3-3	2–5	0.2–1.0	6
PGC1α-1	2–3	0.2–1.0	4
DAX1-2	2–3	0.3–1.8	2
DAX1-3	1–2	0.2–0.4	5
SHP-2	3–9	0.7–1.4	6

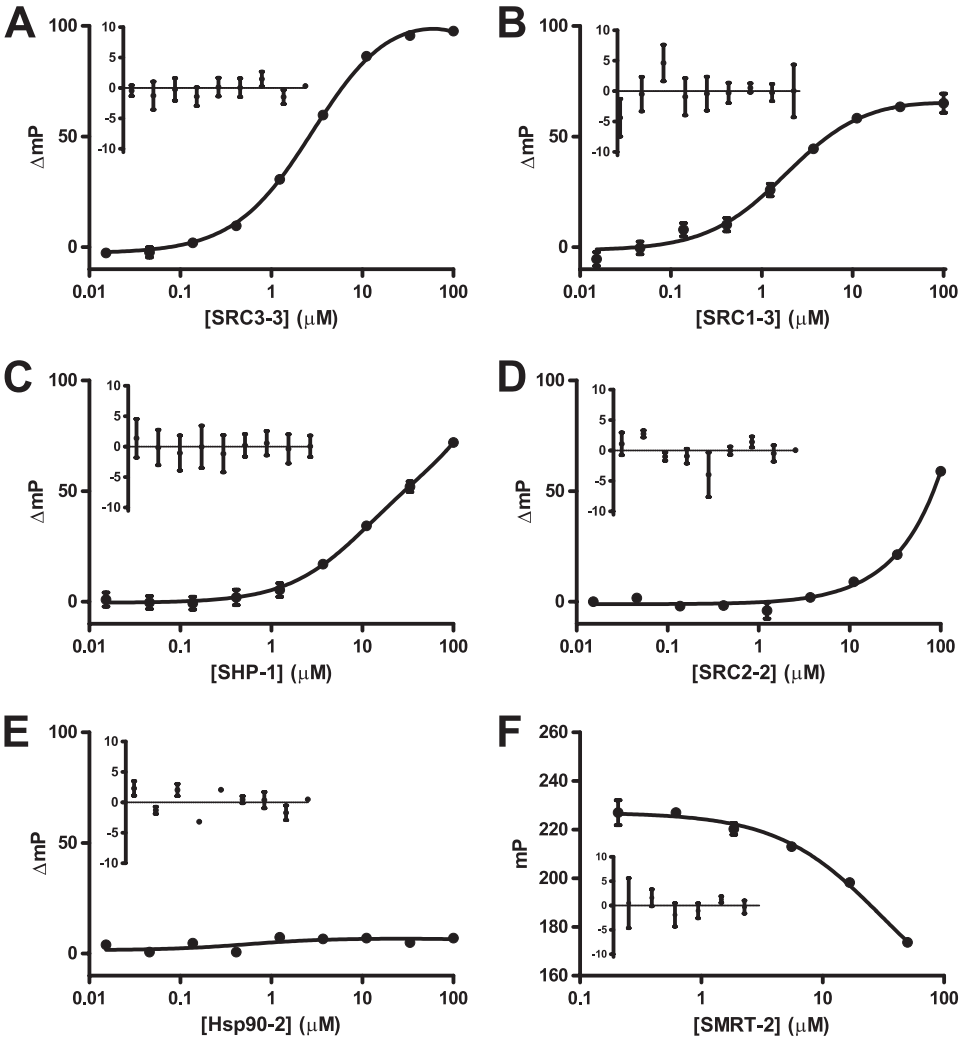

FIGURE 6. **GR binding to NR box peptides by allosteric FP reveals six binding modes.** NR box peptides titrated against 500 nM GR_{SD}, 20 nM dex-fl are shown. *A*, SRC3-3, high plateau saturation is shown. *B*, SRC1-3, low-plateau saturation is shown. *C*, SHP-1, non-saturable binding is shown. *D*, SRC2-2, weak binding is shown. *E*, Hsp90-2, no binding is shown. *F*, SMRT-2, corepressor binding is shown. All data fit to one-site saturation binding model. Residuals shown in the *inset graphs*.

Half-times of association and dissociation of the GR·dex-fl complex, which are NR box-dependent, in both GR contexts were used to cluster the kinetic data for the 18 NR box peptides in our library (Fig. 7). In agreement with the equilibrium data, two primary clusters consisting of 6 binders and 11 non-binders result, with two notable exceptions; DAX1-3, whose exaggerated effects make it an outlier, whereas SRC1-3, found to have a strong affinity for GR in our equilibrium assay, clusters with non-binders due to its weak effect on ligand binding kinetics (Table 1).

SRC1-3 is grouped in the unique low plateau saturable binding mode (Fig. 6*B*). This novel binding mode, characterized by strong affinity (1–2 μM) with a diminished maximum binding signal, can be attributed to SRC1-3 weak effects on ligand binding kinetics (Table 1). By increasing GR·dex-fl association and dissociation half-times only 1- and 2-fold, the tight binding SRC1-3 shows the weakest coupling to the ligand binding pocket. This suggests a transient or passive docking to AF-2 that fails to stabilize this region of the receptor, in stark contrast to the other seven saturable binders, most notably DAX1-3. As previous studies using two-hybrid or peptide competition approaches have reported either moderate (54) or very weak

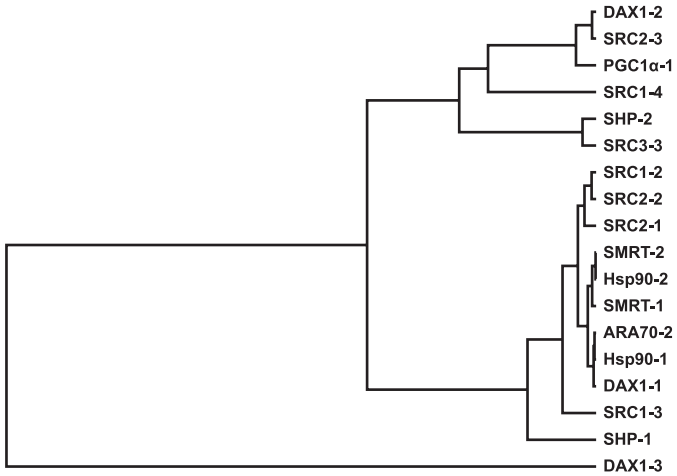

FIGURE 7. **Hierarchical clustering of NR box peptides.** NR box peptides were clustered using half-times shown in Figs. 3 and 4.

	-4	-3	-2	-1	+1	+2	+3	+4	+5	+6	+7
DAX1-3	Q	G	S	I	L	Y	S	L	L	T	S
SRC1-4	Q	K	S	L	L	Q	Q	L	L	T	E
SRC2-3	E	N	A	L	L	R	Y	L	L	D	K
DAX1-2	Q	G	S	I	L	Y	S	M	L	T	S
PGC1α-1	E	P	S	L	L	K	K	L	L	L	A
SRC3-3	N	N	A	L	L	R	Y	L	L	D	R
SHP-2	V	P	S	I	L	K	K	I	L	L	E
SRC1-3	D	H	Q	L	L	R	Y	L	L	D	K

FIGURE 8. **Core sequences of GR binders.** GR binding NR box core sequences with conserved residues are *highlighted*. L*XX*LL Leu residues are in *black*, and GR-specific conserved positions are in *gray*.

(61) interactions between GR and SRC1-3, it is likely that these techniques were not sensitive to the binding mode of SRC1-3.

The co-repressor NR box SMRT-2 displayed a different binding mode (Fig. 6*F*). SMRT-2, not thought to interact with agonist-bound GR, contains the putative co-repressor motif Φ*XX*ΦΦ*XXX*Φ, where Φ is a hydrophobic residue. Co-repressors bind to a structurally modified AF-2 region in which helix 12 is displaced from its active agonist-bound position (77, 78). In contrast with the L*XX*LL-containing NR box peptides, titration of SMRT-2 caused a dose-dependent decrease in polarization of the GR·dex-fl complex. Although saturation was not reached in the assayed concentration range, SMRT-2 appears to act as a low affinity, non-competitive inhibitor of ligand binding. Due to its weak affinity ($IC_{50} > 25$ μM), the biological relevance of this interaction is questionable. However, the ability of GR to interact with SMRT-2 in an agonist-bound context indicates that the receptor has enough intrinsic flexibility to sample conformations capable of binding co-repressors (78).

M752I Increases NR Box Affinity—In addition to its alteration of GR interactions with hormone and Hsp90, the M752I mutation was also shown to produce qualitatively tighter binding of co-activator SRC2 in a pulldown assay (57). The peptides identified as binders to GR_{SD} (Fig. 8) were assayed for binding to GR_{M752I} using a similar experimental setup (supplemental Fig. S2, Table 2). A lower concentration of GR (250 nM as opposed to 500 nM) was used with GR_{M752I} as the binding signal

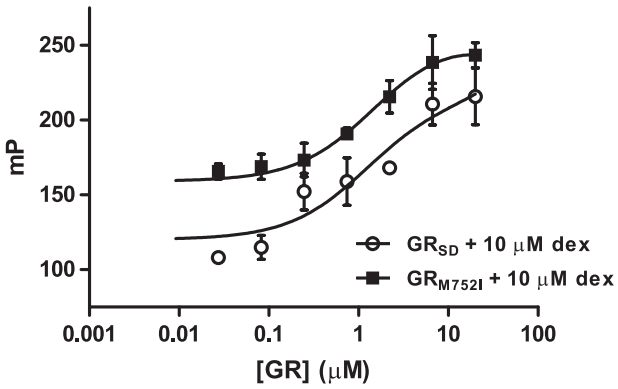

FIGURE 9. **GR binding to SRC1-3-fluor.** GR_{SD} (*open circles*) and GR_{M752I} (*closed squares*) were titrated against 20 nM SRC1-3 conjugated to Alexa-Fluor 555 in the presence of 10 μM dex. Data are fit to a one-site saturation binding model.

was empirically found to be optimal at this concentration. Two distinct behaviors were seen across the eight peptides tested for binding (Table 2). In agreement with the previous study, 7 of 8 NR box peptides showed at least a 2-fold increase in binding affinity as compared with GR_{SD}, whereas the affinity for SRC1-3 remained unchanged. SRC2-3 interaction with GR_{M752I} strengthened most dramatically, with a 7-fold decrease in K_D from GR_{SD}, whereas the strongest interaction remained the DAX1-3-GR interaction, with a K_D of 0.2–0.4 μM.

Characterization of the GR-SRC1-3 Interaction—SRC1-3 emerged as an NR box peptide with novel properties by displaying a relatively strong interaction with GR_{SD} (K_D = 1–2 μM) that did not strengthen upon mutation of Met-752 to Ile but showed weak coupling to ligand binding kinetics, seemingly incongruous with its high affinity (Fig. 3, Table 1). To more fully probe the GR-SRC1-3 interaction, an Alexa Fluor 555-conjugated SRC1-3 peptide was created for direct binding, fluorescence polarization studies. Kinetics of peptide binding were impossible to measure with our assay setup, as the reaction between GR and NR box peptides reached equilibrium within 30 s (data not shown). This finding is in line with surface plasmon resonance-derived kinetics of androgen receptor binding NR box peptides.[5] Steady-state equilibrium binding assays were carried out with both GR constructs and SRC1-3-fluor in the presence of 10 μM dex (Fig. 9). As can be appreciated from the isotherms and accompanying error bars, the interaction between GR and SRC1-3-fluor appears much less stable than the interaction between GR and SRC3-3-fluor (Fig. 5). The high variance observed between duplicate wells is indicative of rapidly shifting molecular populations, which may be the defining feature of the GR-SRC1-3 interaction. SRC1-3 appears to passively dock at the AF-2 surface without coupling to the ligand binding pocket, whereas other interacting NR box peptides dock and effectively register the receptor for ligand binding.

The biological significance of the SRC1-3 binding mode remains to be explored. Few studies have investigated the specific role of SRC1 in GR biology. SRC1a is a splice variant that contains the more typical tight-binding SRC1-4 in addition to SRC1-3 and is an ideal candidate for comparative and muta-

[5] K. Kuchenbecker, unpublished results.

tional studies. Glucocorticoid-dependent global expression analysis of multiple, relevant cell lines in the context of SRC1a with mutations to its NR box regions could provide a valuable clue as to which genes these specific NR boxes are involved in regulating.

DISCUSSION

GR Ligand Binding Pocket and AF-2 Are Allosterically Coupled—An integral step in signal transduction through NRs is the formation of the AF-2 co-regulator binding surface in response to hormone binding. Energetic coupling of these two functional sites has primarily been explored biochemically by manipulating the bound ligand and observing perturbations in the subsequent recruitment pattern of co-regulators to AF-2 (51, 52, 79). In this study we examined the coupling between two of the GR LBD functional sites by fluorescence polarization from the opposite perspective using a fluorescein-labeled GR agonist (*dex-fl*, Fig. 1) and a library of unlabeled co-regulator NR box peptides. The pattern of co-regulator binding to AF-2 was determined using kinetic and equilibrium polarization measurements of dex-fl binding in the ligand binding pocket (Figs. 3, 4, and 6 and supplemental Fig. S1). Of the 18 NR box peptides we examined, 7 showed significant ability to decrease the rates of GR·dex-fl association and dissociation, effectively limiting access to the ligand binding pocket through a kinetic mechanism (Table 1). GR_{SD}·dex-fl association and dissociation were slowed as much as 6- and 27-fold, respectively, in the presence of 10 μM peptide. GR hormone binding in cells is regulated by interactions with Hsp90 chaperone complexes in the cytosol. Co-regulators are not thought to influence the initial hormone binding event, only binding GR after it is transported to the nucleus. However, the observed cooperativity between binding sites reveals a specific functionality of the molecular architecture comprising and connecting AF-2 and the ligand binding pocket. The degree to which this mechanism is shared among NR superfamily members remains mostly unknown and may help to inform future models of differential NR activity. It is also possible that factors regulating other aspects of GR biology are able to exploit the coupling between sites to maintain a hormone-bound state.

DAX1-3 showed by far the greatest effect on hormone binding kinetics, slowing dex-fl dissociation 2-fold more than any other peptide in our library (Table 1). By competing with co-activators for binding at AF-2, DAX1 has been shown to preferentially repress GR-mediated gene activation and not repression (75), a desirable pharmaceutical profile referred to as dissociated. The unique binding mode employed by its third NR box suggests mechanistic details of repression and may represent a new direction for discovery of GR antagonists.

Pattern of Co-regulator Binding to GR AF-2—To more quantitatively assess NR box binding to GR, we employed an equilibrium peptide binding assay, again using unlabeled NR box peptides and dex-fl polarization as the readout (Figs. 6, supplemental Figs. S1 and S2 and Table 2). Binding of the NR box at AF-2 induced a dose-dependent increase in dex-fl polarization, resulting from the ability of the peptide to slow both ligand association and dissociation. Six distinct binding modes were observed among the 18 NR box peptides in our library, with 8 of the peptides showing saturation binding behavior (Figs. 6, supplemental Fig. S1 and Table 2). The core sequences of these eight NR box peptides, for which K_Ds could be determined, are shown in Fig. 8. Aside from the conserved leucine residues of the L*XX*LL motif, these peptides show significant conservation at three additional sites, suggesting a more complete consensus sequence for high affinity binding to GR AF-2. The conserved hydrophobic residue at the −1 position, directly preceding L*XX*LL, has been appreciated as a key component of NR box binding to several NRs (50), and indeed all eight binders contain Leu or Ile here. The data presented here reveal that 7 of 8 binders have Ala or Ser at the −2 position, indicating a preference for residues with small side chains at this position. As structural alignments of GR·NR box complexes do not indicate a role for this residue in direct AF-2 recognition, it may contribute to binding by allowing the NR box to attain a conformation appropriate for docking. Interestingly, the non-canonical binder SRC1-3 has a Gln here, which may contribute to the novel binding mode employed by this NR box. The −4 position is also well conserved, with a branched, polar residue (Glu, Gln, Asp, Asn) appearing in seven of eight binders. These four amino acid side chains would be expected to be solvent-exposed as they are among the most polar of side chains. In the GR·dex·SRC2-3 crystal structure, this residue favorably packs against Asn-759, Asp in the most closely related mineralocorticoid receptor, Ala and Val, respectively, in the progesterone and androgen receptors, indicating a role for the −4 position in specific co-regulator recognition of the corticosteroid sub-class of SRs.

M752I Alters Both Ligand and Peptide Interactions with GR—The mechanism of co-regulator binding was also determined for GR with the mutation M752I (Figs 4, supplemental Fig. S2, and Tables 1 and 2). This mutation was shown to increase GR affinity for co-regulators binding at AF-2 while decreasing the receptor dependence on Hsp90 (57). The results of our equilibrium binding assay verify this finding, with seven of eight GR_{SD}-binding peptides showing increased affinity for GR_{M752I} (Table 2). SRC1-3 was the lone NR box peptide whose affinity failed to increase, solidifying its status as an atypical binder. Co-regulator modulation of dex-fl binding kinetics was also observed for GR_{M752I} (Fig. 4, Table 1). Interestingly, the two versions of GR behaved differently. Our analysis of peptide regulation of GR_{M752I}·dex-fl complex formation showed interacting NR box peptides to have a similar effect on both on and off rates for the ligand, whereas for GR_{SD}·dex-fl we found that NR box peptides preferentially influenced off rates (Figs. 3 and 4, Table 1). These results suggest two mechanisms, one direct, the other indirect, underlying the binding to M752I. In the direct mechanism (1) the strategically positioned Ile increases peptide affinity for the unliganded receptor, with a kinetic effect solely dependent on peptide residence time at AF-2. In the indirect mechanism (2) the Ile alters the coupling between AF-2 and the ligand binding pocket by introducing a more

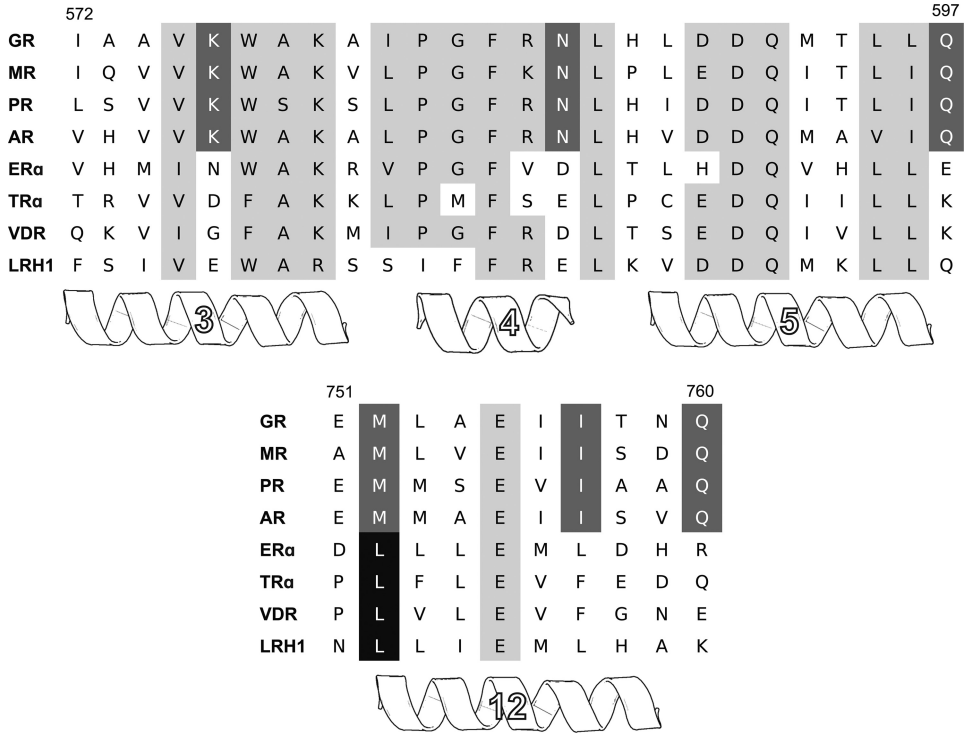

FIGURE 10. **Sequence alignment of NR AF-2 regions.** NR LBD crystal structures were aligned in PyMOL. Residues conserved across the NR superfamily are in *light gray*. Residues conserved among SRs are in *dark gray*. Residues conserved among non-SRs are in *black*. The Protein Data Bank codes of structures used for the alignment are GR (3BQD), mineralocorticoid receptor (*MR*) (2ABI), progesterone receptor (*PR*) (3D90), androgen receptor (1T7R), ER (2OCF), vitamin D receptor (*VDR*) (2ZL9), thyroid hormone receptor (*TR*) (3HZF), LRH-1 (1YOK).

rigid side chain into the allosteric network. We demonstrated by direct measurement of peptide binding that a representative NR box, SRC3-3, has nearly identical affinities for dex-bound and apoGR suggesting mechanism (2) (Fig. 5).

This leads to a view of Met-752 as a two-way molecular sensor whose flexible side chain allows hormone association at a reduced rate to GR with an NR box, or presumably a co-regulator, bound at AF-2. Mutation to Ile strengthens the GR interactions with NR box peptides while dramatically slowing hormone association with peptide bound, indicating that the ligand binding pocket can no longer signal that it is empty. It is likely that disruption of this vital intraprotein communication mechanism in this manner would greatly compromise signaling through GR by effectively eliminating hormone binding as a prerequisite for receptor function.

The AF-2 surface and its surrounding residues are well conserved throughout the nuclear receptor superfamily. Sequence alignment of the SR family with representative NRs from the other classes reveals several AF-2 residues that are conserved across the superfamily and six, including Met-752, that are conserved among SRs with the exception of ER (Fig. 10). At these six positions, the only residue that is conserved in the non-SRs as well is Leu at the position corresponding to Met-752 in GR. Receptors containing Leu here, including ER, vitamin D receptor, thyroid hormone receptor, and retinoic acid receptor, are regulated in a dramatically different fashion from the canonical SRs. Typically, they do not depend on Hsp90 and are localized to the nucleus in the absence of hormone, two behaviors induced by the M752I mutation in GR (57). ER is the only receptor bearing a Leu here to show dependence on Hsp90. However, the Hsp90-ER interaction is less dependent on the ER LBD than other SRs, and ER can readily translocate to the nucleus in the absence of hormone (80, 81). Our results indicate the 752 position as a key regulator of the allosteric network connecting hormone and co-regulator binding sites in GR LBD. Conservation of this residue among Hsp90-dependent receptors and the functional consequences of mutations that rigidify the position suggest evolutionary pressure toward flexibility at this site in SRs. The mechanisms by which this flexibility is recognized and exploited by Hsp90 and other regulatory elements remain unclear.

GR is a finely tuned molecular switch capable of carrying out a myriad of critical functions at the organismal level. As a ligand-regulated scaffolding molecule, GR must translate extrinsic hormone signals into a meaningful conformational change to promote interactions with chaperones, DNA, and a variety of co-regulator proteins. These interactions, across all of GR domains, determine the outcome of a GC signal. This study and others have aimed to provide a quantitative framework for the description of these interactions and the allosteric mechanisms by which they are enabled (26). Recent advances in the purification and structural characterization of multidomain NR constructs should enable this work to be extended into molecules of absolute biological relevance and increasing complexity (82, 83).

Acknowledgments—We thank C. Cunningham, J. Dilla, C. Farady, E. Kirschke, and K. Kuchenbecker for helpful scientific discussions.

REFERENCES

1. Katzenellenbogen, B. S. (1980) *Annu. Rev. Physiol.* **42,** 17–35
2. Chrousos, G. P., and Kino, T. (2007) *Stress* **10,** 213–219
3. Rhen, T., and Cidlowski, J. A. (2005) *N. Engl. J. Med.* **353,** 1711–1723
4. Chrousos, G. P., Charmandari, E., and Kino, T. (2004) *J. Clin. Endocrinol. Metab.* **89,** 563–564
5. Pratt, W. B., and Dittmar, K. D. (1998) *Trends Endocrinol. Metab.* **9,** 244–252
6. Hutchison, K. A., Dittmar, K. D., and Pratt, W. B. (1994) *J. Biol. Chem.* **269,** 27894–27899
7. Picard, D., Khursheed, B., Garabedian, M. J., Fortin, M. G., Lindquist, S., and Yamamoto, K. R. (1990) *Nature* **348,** 166–168
8. Pratt, W. B., Galigniana, M. D., Morishima, Y., and Murphy, P. J. (2004) *Essays Biochem.* **40,** 41–58
9. Bresnick, E. H., Dalman, F. C., Sanchez, E. R., and Pratt, W. B. (1989) *J. Biol. Chem.* **264,** 4992–4997

10. Echeverría, P. C., Mazaira, G., Erlejman, A., Gomez-Sanchez, C., Piwien, Pilipuk, G., and Galigniana, M. D. (2009) *Mol. Cell. Biol.* **29,** 4788–4797
11. Picard, D., and Yamamoto, K. R. (1987) *EMBO J.* **6,** 3333–3340
12. Tanaka, M., Nishi, M., Morimoto, M., Sugimoto, T., and Kawata, M. (2003) *Endocrinology* **144,** 4070–4079
13. Htun, H., Barsony, J., Renyi, I., Gould, D. L., and Hager, G. L. (1996) *Proc. Natl. Acad. Sci. U.S.A.* **93,** 4845–4850
14. Rogatsky, I., Wang, J. C., Derynck, M. K., Nonaka, D. F., Khodabakhsh, D. B., Haqq, C. M., Darimont, B. D., Garabedian, M. J., and Yamamoto, K. R. (2003) *Proc. Natl. Acad. Sci. U.S.A.* **100,** 13845–13850
15. Galon, J., Franchimont, D., Hiroi, N., Frey, G., Boettner, A., Ehrhart-Bornstein, M., O'Shea, J. J., Chrousos, G. P., and Bornstein, S. R. (2002) *FASEB J.* **16,** 61–71
16. John, S., Johnson, T. A., Sung, M. H., Biddie, S. C., Trump, S., Koch-Paiz, C. A., Davis, S. R., Walker, R., Meltzer, P. S., and Hager, G. L. (2009) *Endocrinology* **150,** 1766–1774
17. Stavreva, D. A., Müller, W. G., Hager, G. L., Smith, C. L., and McNally, J. G. (2004) *Mol. Cell. Biol.* **24,** 2682–2697
18. McNally, J. G., Müller, W. G., Walker, D., Wolford, R., and Hager, G. L. (2000) *Science* **287,** 1262–1265
19. Biddie, S. C., and Hager, G. L. (2009) *Stress* **12,** 193–205
20. Iñiguez-Lluhí, J. A., Lou, D. Y., and Yamamoto, K. R. (1997) *J. Biol. Chem.* **272,** 4149–4156
21. Wärnmark, A., Gustafsson, J. A., and Wright, A. P. (2000) *J. Biol. Chem.* **275,** 15014–15018
22. Baumann, H., Paulsen, K., Kovács, H., Berglund, H., Wright, A. P., Gustafsson, J. A., and Härd, T. (1993) *Biochemistry* **32,** 13463–13471
23. Luisi, B. F., Xu, W. X., Otwinowski, Z., Freedman, L. P., Yamamoto, K. R., and Sigler, P. B. (1991) *Nature* **352,** 497–505
24. Härd, T., Kellenbach, E., Boelens, R., Maler, B. A., Dahlman, K., Freedman, L. P., Carlstedt-Duke, J., Yamamoto, K. R., Gustafsson, J. A., and Kaptein, R. (1990) *Science* **249,** 157–160
25. Kumar, R., and Thompson, E. B. (2005) *J Steroid Biochem. Mol. Biol.* **94,** 383–394
26. Meijsing, S. H., Pufall, M. A., So, A. Y., Bates, D. L., Chen, L., and Yamamoto, K. R. (2009) *Science* **324,** 407–410
27. Ortlund, E. A., Bridgham, J. T., Redinbo, M. R., and Thornton, J. W. (2007) *Science* **317,** 1544–1548
28. Bridgham, J. T., Ortlund, E. A., and Thornton, J. W. (2009) *Nature* **461,** 515–519
29. Bridgham, J. T., Carroll, S. M., and Thornton, J. W. (2006) *Science* **312,** 97–101
30. Wagner, R. L., Apriletti, J. W., McGrath, M. E., West, B. L., Baxter, J. D., and Fletterick, R. J. (1995) *Nature* **378,** 690–697
31. Renaud, J. P., Rochel, N., Ruff, M., Vivat, V., Chambon, P., Gronemeyer, H., and Moras, D. (1995) *Nature* **378,** 681–689
32. Bourguet, W., Ruff, M., Chambon, P., Gronemeyer, H., and Moras, D. (1995) *Nature* **375,** 377–382
33. Mangelsdorf, D. J., and Evans, R. M. (1995) *Cell* **83,** 841–850
34. Darimont, B. D., Wagner, R. L., Apriletti, J. W., Stallcup, M. R., Kushner, P. J., Baxter, J. D., Fletterick, R. J., and Yamamoto, K. R. (1998) *Genes Dev.* **12,** 3343–3356
35. Feng, W., Ribeiro, R. C., Wagner, R. L., Nguyen, H., Apriletti, J. W., Fletterick, R. J., Baxter, J. D., Kushner, P. J., and West, B. L. (1998) *Science* **280,** 1747–1749
36. Shiau, A. K., Barstad, D., Loria, P. M., Cheng, L., Kushner, P. J., Agard, D. A., and Greene, G. L. (1998) *Cell* **95,** 927–937
37. McKenna, N. J., Lanz, R. B., and O'Malley, B. W. (1999) *Endocr. Rev.* **20,** 321–344
38. McKenna, N. J., and O'Malley, B. W. (2002) *Cell* **108,** 465–474
39. Xu, J., and Li, Q. (2003) *Mol. Endocrinol.* **17,** 1681–1692
40. Hong, H., Kohli, K., Trivedi, A., Johnson, D. L., and Stallcup, M. R. (1996) *Proc. Natl. Acad. Sci. U.S.A.* **93,** 4948–4952
41. Voegel, J. J., Heine, M. J., Zechel, C., Chambon, P., and Gronemeyer, H. (1996) *EMBO J.* **15,** 3667–3675
42. Zhu, Y., Qi, C., Calandra, C., Rao, M. S., and Reddy, J. K. (1996) *Gene Expr.* **6,** 185–195
43. Chen, J. D., Umesono, K., and Evans, R. M. (1996) *Proc. Natl. Acad. Sci. U.S.A.* **93,** 7567–7571
44. Belandia, B., and Parker, M. G. (2003) *Cell* **114,** 277–280
45. Fryer, C. J., and Archer, T. K. (1998) *Nature* **393,** 88–91
46. Heery, D. M., Kalkhoven, E., Hoare, S., and Parker, M. G. (1997) *Nature* **387,** 733–736
47. Voegel, J. J., Heine, M. J., Tini, M., Vivat, V., Chambon, P., and Gronemeyer, H. (1998) *EMBO J.* **17,** 507–519
48. Hong, H., Kohli, K., Garabedian, M. J., and Stallcup, M. R. (1997) *Mol. Cell. Biol.* **17,** 2735–2744
49. Onate, S. A., Boonyaratanakornkit, V., Spencer, T. E., Tsai, S. Y., Tsai, M. J., Edwards, D. P., and O'Malley, B. W. (1998) *J. Biol. Chem.* **273,** 12101–12108
50. Chang, C., Norris, J. D., Grøn, H., Paige, L. A., Hamilton, P. T., Kenan, D. J., Fowlkes, D., and McDonnell, D. P. (1999) *Mol. Cell. Biol.* **19,** 8226–8239
51. Moore, J. M., Galicia, S. J., McReynolds, A. C., Nguyen, N. H., Scanlan, T. S., and Guy, R. K. (2004) *J. Biol. Chem.* **279,** 27584–27590
52. Teichert, A., Arnold, L. A., Otieno, S., Oda, Y., Augustinaite, I., Geistlinger, T. R., Kriwacki, R. W., Guy, R. K., and Bikle, D. D. (2009) *Biochemistry* **48,** 1454–1461
53. Bramlett, K. S., Wu, Y., and Burris, T. P. (2001) *Mol. Endocrinol.* **15,** 909–922
54. Wu, J., Li, Y., Dietz, J., and Lala, D. S. (2004) *Mol. Endocrinol.* **18,** 53–62
55. Hur, E., Pfaff, S. J., Payne, E. S., Grøn, H., Buehrer, B. M., and Fletterick, R. J. (2004) *PLoS Biol.* **2,** E274
56. Estébanez-Perpiñá, E., Moore, J. M., Mar, E., Delgado-Rodrigues, E., Nguyen, P., Baxter, J. D., Buehrer, B. M., Webb, P., Fletterick, R. J., and Guy, R. K. (2005) *J. Biol. Chem.* **280,** 8060–8068
57. Ricketson, D., Hostick, U., Fang, L., Yamamoto, K. R., and Darimont, B. D. (2007) *J. Mol. Biol.* **368,** 729–741
58. Kroe, R. R., Baker, M. A., Brown, M. P., Farrow, N. A., Gautschi, E., Hopkins, J. L., LaFrance, R. R., Kronkaitis, A., Freeman, D., Thomson, D., Nabozny, G., Grygon, C. A., and Labadia, M. E. (2007) *Biophys. Chem.* **128,** 156–164
59. Bledsoe, R. K., Montana, V. G., Stanley, T. B., Delves, C. J., Apolito, C. J., McKee, D. D., Consler, T. G., Parks, D. J., Stewart, E. L., Willson, T. M., Lambert, M. H., Moore, J. T., Pearce, K. H., and Xu, H. E. (2002) *Cell* **110,** 93–105
60. Kauppi, B., Jakob, C., Färnegårdh, M., Yang, J., Ahola, H., Alarcon, M., Calles, K., Engström, O., Harlan, J., Muchmore, S., Ramqvist, A. K., Thorell, S., Ohman, L., Greer, J., Gustafsson, J. A., Carlstedt-Duke, J., and Carlquist, M. (2003) *J. Biol. Chem.* **278,** 22748–22754
61. Suino-Powell, K., Xu, Y., Zhang, C., Tao, Y. G., Tolbert, W. D., Simons, S. S., Jr., and Xu, H. E. (2008) *Mol. Cell. Biol.* **28,** 1915–1923
62. Biggadike, K., Bledsoe, R. K., Hassell, A. M., Kirk, B. E., McLay, I. M., Shewchuk, L. M., and Stewart, E. L. (2008) *J. Med. Chem.* **51,** 3349–3352
63. Madauss, K. P., Bledsoe, R. K., Mclay, I., Stewart, E. L., Uings, I. J., Weingarten, G., and Williams, S. P. (2008) *Bioorg. Med. Chem. Lett.* **18,** 6097–6099
64. Frego, L., and Davidson, W. (2006) *Protein Sci.* **15,** 722–730
65. Lin, S., Bock, C. L., Gardner, D. B., Webster, J. C., Favata, M. F., Trzaskos, J. M., and Oldenburg, K. R. (2002) *Anal. Biochem.* **300,** 15–21
66. Gee, A. C., Carlson, K. E., Martini, P. G., Katzenellenbogen, B. S., and Katzenellenbogen, J. A. (1999) *Mol. Endocrinol.* **13,** 1912–1923
67. Kallenberger, B. C., Love, J. D., Chatterjee, V. K., and Schwabe, J. W. (2003) *Nat. Struct. Biol.* **10,** 136–140
68. Pérez Santín, E., Germain, P., Quillard, F., Khanwalkar, H., Rodríguez-Barrios, F., Gronemeyer, H., de Lera, A. R., and Bourguet, W. (2009) *J. Med. Chem.* **52,** 3150–3158
69. Nahoum, V., Pérez, E., Germain, P., Rodríguez-Barrios, F., Manzo, F., Kammerer, S., Lemaire, G., Hirsch, O., Royer, C. A., Gronemeyer, H., de Lera, A. R., and Bourguet, W. (2007) *Proc. Natl. Acad. Sci. U.S.A.* **104,** 17323–17328
70. Li, Y., Suino, K., Daugherty, J., and Xu, H. E. (2005) *Mol. Cell* **19,** 367–380
71. He, B., Kemppainen, J. A., Voegel, J. J., Gronemeyer, H., and Wilson, E. M. (1999) *J. Biol. Chem.* **274,** 37219–37225
72. Dalman, F. C., Koenig, R. J., Perdew, G. H., Massa, E., and Pratt, W. B. (1990) *J. Biol. Chem.* **265,** 3615–3618
73. Dalman, F. C., Sturzenbecker, L. J., Levin, A. A., Lucas, D. A., Perdew,

G. H., Petkovitch, M., Chambon, P., Grippo, J. F., and Pratt, W. B. (1991) *Biochemistry* **30,** 5605–5608
74. Sablin, E. P., Woods, A., Krylova, I. N., Hwang, P., Ingraham, H. A., and Fletterick, R. J. (2008) *Proc. Natl. Acad. Sci. U.S.A.* **105,** 18390–18395
75. Zhou, J., Oakley, R. H., and Cidlowski, J. A. (2008) *Mol Endocrinol* **22,** 1521–1534
76. Borgius, L. J., Steffensen, K. R., Gustafsson, J. A., and Treuter, E. (2002) *J. Biol. Chem.* **277,** 49761–49766
77. Xu, H. E., Stanley, T. B., Montana, V. G., Lambert, M. H., Shearer, B. G., Cobb, J. E., McKee, D. D., Galardi, C. M., Plunket, K. D., Nolte, R. T., Parks, D. J., Moore, J. T., Kliewer, S. A., Willson, T. M., and Stimmel, J. B. (2002) *Nature* **415,** 813–817
78. Madauss, K. P., Grygielko, E. T., Deng, S. J., Sulpizio, A. C., Stanley, T. B., Wu, C., Short, S. A., Thompson, S. K., Stewart, E. L., Laping, N. J., Williams, S. P., and Bray, J. D. (2007) *Mol. Endocrinol.* **21,** 1066–1081
79. Moore, J. M., and Guy, R. K. (2005) *Mol. Cell. Proteomics* **4,** 475–482
80. Schlatter, L. K., Howard, K. J., Parker, M. G., and Distelhorst, C. W. (1992) *Mol. Endocrinol.* **6,** 132–140
81. Picard, D., Kumar, V., Chambon, P., and Yamamoto, K. R. (1990) *Cell Regul.* **1,** 291–299
82. Chandra, V., Huang, P., Hamuro, Y., Raghuram, S., Wang, Y., Burris, T. P., and Rastinejad, F. (2008) *Nature* **456,** 350–356
83. Simmons, C. A., Bledsoe, R. K., Guex, N., and Pearce, K. H. (2008) *Protein Expr. Purif.* **62,** 29–35